Water Air Soil Pollut (2020) 231: 472
https://doi.org/10.1007/s11270-020-04820-7

Generation of Alkalinity by Stimulation of Microbial Iron Reduction in Acid Rock Drainage Systems: Impact of Natural Organic Matter Types

Martha E. Jimenez-Castaneda · Carolina Scarinci · Adam Burke · Christopher Boothman · David J. Vaughan · Jonathan R. Lloyd · Bart E. van Dongen

Received: 8 April 2020 / Accepted: 13 August 2020 / Published online: 31 August 2020

Abstract To determine the role of organic matter in the attenuation of acid rock drainage (ARD), microcosm-based experiments were performed using ARD stimulated with plants and manures. Initial mineralogical, organic geochemical and microbial analyses indicated a predominance of goethite, a substantial amount of organic carbon originating from local sources, and a bacterial community comparable with those detected in a range of ARD sites worldwide. After 100 days of incubation, changes in the mineralogical, organic and microbiological composition of the ARD demonstrated that the plant additions stimulate microbes with the potential to degrade this organic matter but do not necessarily cause substantial Fe(III) reduction. Conversely, the greatest observed stimulation of Fe(III) reduction, associated with an increase in pH to near-neutral values, was observed using manure additions. These results demonstrate that the use of the optimal natural carbon source is important and can promote the metabolism of microorganisms potentially fuelling a range of geomicrobial processes, including iron and sulfate reduction.

Keywords ARD · Geochemistry · Organic matter · Remediation

1 Introduction

Acid mine drainage (AMD) is one of the most widespread forms of water pollution in the world characterised by surface waters with low pH and elevated concentrations of iron, other dissolved metals and sulfuric acid (Singer and Stumm 1970; Rimstidt and Vaughan 2003). This phenomenon is commonly associated with environmental disasters from mine spills but can also arise from natural sources and is then known as acid rock drainage, ARD (Liao et al. 2016; Queiroz et al. 2018; Moeng 2019). In most passive ARD treatments, alkalinity generated via sulfate reduction coupled with organic matter oxidation is preferred (Costa and Duarte 2005; Williamson et al. 2013; Kim et al. 2014), but other anaerobic processes that can generate alkalinity, such as microbial Fe(III) reduction, have not been studied as extensively.

Electronic supplementary material The online version of this article (https://doi.org/10.1007/s11270-020-04820-7) contains supplementary material, which is available to authorized users.

M. E. Jimenez-Castaneda · C. Scarinci · A. Burke ·
C. Boothman · D. J. Vaughan · J. R. Lloyd ·
B. E. van Dongen (✉)
School of Earth and Environmental Sciences, and Williamson Research Centre for Molecular Environmental Science, University of Manchester, Manchester, UK
e-mail: bart.vandongen@manchester.ac.uk

Present Address:
M. E. Jimenez-Castaneda
Department of Earth, Atmospheric and Planetary Sciences, Purdue University, West Lafayette, IN, USA

Iron minerals formed from pyrite oxidation can be used as substrate for this form of anaerobic respiration (Johnson 1998; Cutting et al. 2009). Microbial Fe(III) reduction may occur in anaerobic sediments under acidic conditions, coupled to the oxidation of organic matter (Lovley and Phillips 1986). Adams et al. (2007) showed that the addition of glycerol and complex electron donors to ARD sediments stimulates the microbial reduction of Fe(III), leading to an increase in pH. Natural sources of organic matter may also stimulate alkali-generating processes such as Fe(III) reduction, although to what extent the bioavailability of the organic matter can drive the attenuation of ARD remains unclear.

So as to investigate these processes, Fe(III)-rich sediments from an ARD site were used in microcosm-based experiments involving a range of natural carbon sources as potential electron donors. The mineralogical and geochemical transformations taking place, as well as the microbial communities present before and after 100 days of incubation, were determined to investigate the influence of natural carbon sources on the stimulation of Fe(III) reduction and hence the contribution to the ARD attenuation.

2 Materials and Analytical Methods

2.1 Study Site and Sample Collection

The Mam Tor landslide (Castleton, Derbyshire, UK; Fig. 1) has caused the continuing exposure of the iron-rich rocks for over 3200 years (Vear and Curtis 1981; Waltham and Dixon 2000; Rutter and Green 2011). Due to the continuous exposure of iron-rich rocks to rainfall, several ARD ponds have formed near the bottom of the landslide hosting a range of Fe(III)-reducing bacteria (Adams et al. 2007). More information about the study site can be found in the supplemental material.

Sediment samples from one of these ponds rich in Fe(III) minerals (Fig. 1) were collected using a stainless steel scoop and transferred into clean glass jars. Samples of local plants such as reeds, ferns and *Sphagnum* moss were collected into pre-furnaced aluminium foil bags; acidic pond water (pH ~ 3) was also collected using clean plastic bottles. Manure samples were collected using clean glass jars at Mam Tor (sheep manure) and at Tatton Park, Cheshire, UK (pig and cow manure). The sediment and water samples were stored in the dark at − 4 °C to

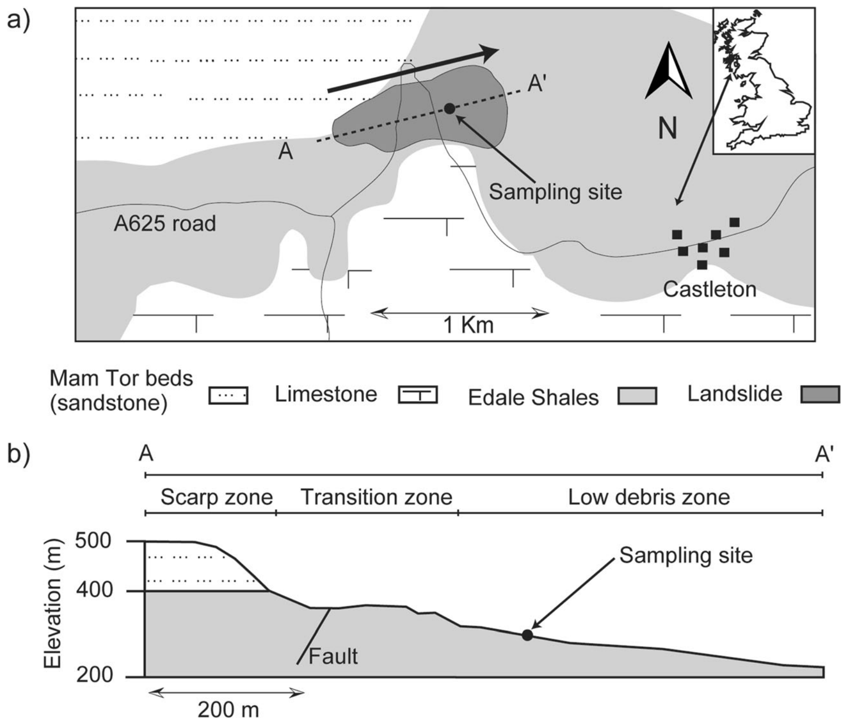

Fig. 1 **a** Location map and relevant geology of the Mam Tor landslide and **b** the cross section A-A′ shows the Mam Tor beds and the Edale Shales; the scarp zone, transition zone and low debris zone of the landslide are also indicated. The bold arrow indicates the general direction of the landslide (figure modified from Skempton et al. 1989 and Waltham and Dixon 2000)

minimise any microbial activity. Plant and manure samples were stored at − 20 °C until further analyses.

2.2 Microcosm Experiments

Six sets of microcosm experiments were set up in quadruplicate, using 100-ml sterile serum bottles with 30 g of sediment, 60 ml of acidic pond water and 1 g of either plant or manure as carbon sources and electron donors for anaerobic processes. Two control experiments were set up in triplicate using the same ratio of sediment to water, and either glycerol (50 mM) added as a readily bioavailable carbon source and electron donor in positive controls (Adams et al. 2007) or without addition of any external carbon source (an 'unamended' microcosm). All microcosm bottles were sealed using butyl rubber stoppers and aluminium clamps, and bubbled with nitrogen for 15 min to ensure anaerobic conditions. Three out of four microcosms were incubated at 20 °C for 100 days; the fourth microcosm of each series was sampled immediately for measurement of pH, Eh and iron content, and stored after sampling at − 20 °C to preserve the initial conditions (initial samples). Slurry samples of the incubated microcosms were taken under anaerobic conditions after 0, 7, 14, 28, 50 and 100 days of incubation for pH and Eh measurements using a Basic Denver pH/ORP meter (Denver Instrument Company) with a 3M KCl liquid-filled electrode (Ag/AgCl reference). Subsamples were filtered (0.22 μm) and acidified (2% *w*/*v*, HNO_3) for elemental analysis on an Optima 5300 dual view ICP-AES (PerkinElmer, USA) and the concentrations of short-chain acids, such as acetate and lactate, were determined by ion chromatography on filtered subsamples (0.22 μm) using a Bio High Pressure Liquid Chromatograph (Dionex, USA) equipped with an IonPac ICE-AS1 ion-exclusion column (Dionex, USA). The bioavailable soluble Fe(II) was measured in triplicate at the same sampling times, using the ferrozine assay procedure (Stookey 1970), reading the optical absorbance (at 562 nm) using a Jenway 6715 UV/visible spectrophotometer. After incubation for 100 days and pH, Eh and iron content measurements, subsamples for microbial analyses were collected and stored at − 80 °C. Afterwards, a composed sample was prepared using the remaining slurries of each experiment and subsamples were obtained and dried anaerobically for Mössbauer analyses. The remaining slurries were freeze dried and used for other analyses.

2.3 Mineralogical, Geochemical and Microbial Analyses

The mineralogy and geochemistry of the ARD sediment and microcosm slurries were monitored using ^{57}Fe Mössbauer spectroscopy, X-ray (powder) diffraction (XRD) and X-ray fluorescence (XRF) analyses and the total organic matter content was quantified using the sequential loss on ignition method (Heiri et al. 2001, Beaudoin 2003; see supplemental material for details). For lipid analyses, freeze-dried and homogenised ARD sediment (40 g), microcosm slurries (5 g) and local vegetation or manures (1 g) were extracted using a Soxhlet apparatus for 24 h with a solution of dichloromethane/methanol (2:1; *v*/*v*). The total lipid extracts obtained were fractionated using the method described by Dickson et al. (2009). After the removal of elemental sulfur (Blumer 1957), the extracts were derivatised and analysed by gas chromatography mass spectrometry (GC-MS; see supplemental material for details). To determine whether macromolecular (lignocellulosic) organic matter from the plant and manure enrichments was used during incubation, residues of the extracted samples were analysed by pyrolysis GC-MS (Py-GC-MS; see supplemental material for details). To identify the bacteria 'biostimulated' with the organic carbon additions, and to investigate their potential capacity for coupling Fe(III) reduction to the oxidation of organic matter, the bacterial diversity of the ARD sediment/slurries before (initial time) and after incubation (100 days) was studied by sequence analysis of PCR amplified 16S ribosomal RNA genes (16S rRNA; Bassil et al. 2015; see supplemental material for details).

3 Results and Discussions

3.1 Mineralogical and Geochemical Characterisation of ARD Sediment

The XRF analysis of the ARD sediment (Table S1) showed a predominance of iron reported here as Fe_2O_3 (89%) and sulfur reported as SO_3 (8.4%) with minor amounts of other elements, probably associated with phyllosilicates (Allen 1960; Ford et al. 1993), while

XRD analyses and Mössbauer spectroscopy showed a dominance of goethite (Fig. 2a). At room temperature (Fig. 2b), the Mössbauer spectrum of the ARD sediment was fitted using a single doublet identified as goethite (δ/Fe = 0.38 mm/s; Δ = 0.56 mm/s; see Table 1 for explanation of parameters). At liquid nitrogen temperature (Fig. 2b; Table 1), the spectrum was fitted with two six-line patterns with different hyperfine magnetic field values. The value of 462 kOe (δ/Fe = 0.49 mm/s) is probably from goethite (Eissa et al. 1974; Murad 1989; Bocquet et al. 1992). The smaller value of 431 kOe (δ/Fe = 0.48 mm/s) could originate from one of two possible causes: an impure goethite (with an impurity such as Al) or an effect arising from small particle sizes (van der Kraan and van Loef 1966; Golden et al. 1979; Mørup et al. 1982; Bocquet et al. 1992). A central doublet (δ/Fe = 0.46 mm/s, Δ = 0.73 mm/s) was also observed in the Mössbauer spectrum and was attributed to fine-particle goethite (Larese-Casanova et al. 2010), in line with the earlier observations of the smaller hyperfine magnetic field value subspectrum, the crystallite size (40.1 ± 3.5 nm) calculated from XRD using the Scherrer relation and the low aluminium content of the sediment (0.5%).

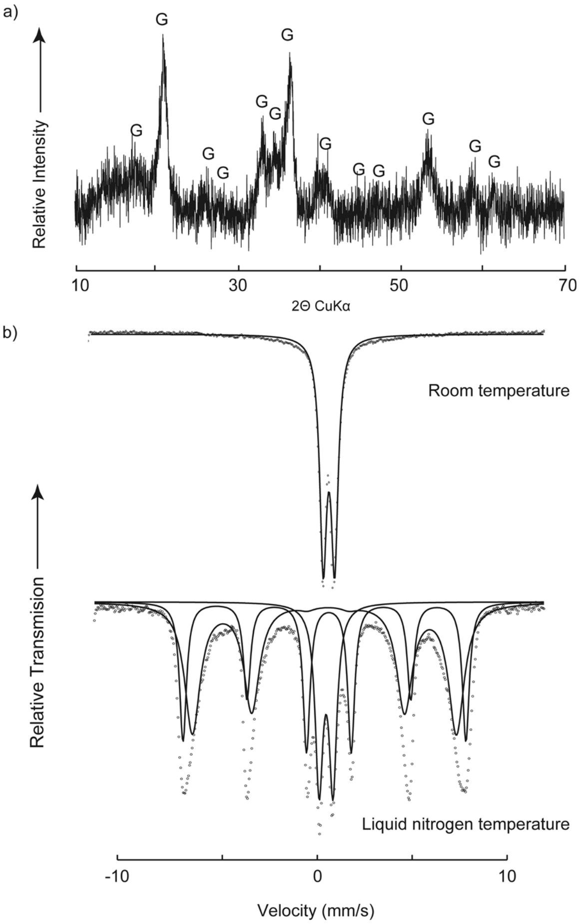

Fig. 2 **a** X-ray diffractogram (XRD) showing goethite (G) as the dominant mineral phase and **b** Mössbauer spectra of Mam Tor ARD sediment. The Mössbauer spectrum at room temperature is comprised of a single doublet interpreted as being from goethite. At liquid nitrogen temperature, the spectrum shows the behaviour expected from goethite with sextets arising from magnetic ordering and with a central doublet produced by the superparamagnetism due to a contribution from very small size particles of goethite

Organic geochemical analyses demonstrated the presence of substantial amounts of organic matter (14%) indicating that the site is not carbon limited. Lipid analyses of the ARD sediment and higher plant vegetation further suggest inputs from a mix of plants with a predominant contribution of *Sphagnum* moss (Table S2 and Fig. S1a; see supplemental material for details). Macromolecular analyses of the ARD sediment indicated a macromolecular composition dominated by a relatively high contribution of polysaccharides (44%), a substantial amount of lignin products (19%), nitrogen compounds (17%), phenols (12%) and aromatic compounds (7%; Fig. S1b). Comparing the macromolecular composition of the ARD sediments with those of the plants again suggests a mixed plant input into the sediment, with a predominant contribution of *Sphagnum* moss, supporting the lipid analyses (Fig. S1b). In summary, the ARD sediment was dominated by goethite with a substantial amount of organic carbon originating from local plants, mainly moss. However, whether the plant-derived organic components are bioavailable to the extant microbial community, including bacteria able to respire Fe(III) in the sediments potentially leading to ARD amelioration, was investigated using microcosm experiments described below.

3.2 The Bacterial Community Before Biostimulation

The 16S rRNA gene sequences of the bacteria inhabiting the ARD were amplified and sequenced to provide microbial baseline data, which could later be compared with the bacterial community after biostimulation with organic carbon. Four main phylogenetic divisions (Fig. 3) were identified in the sediment (*Solibacteres*, *Alphaproteobacteria*, *Gammaproteobacteria* and *Acidobacteria*) with a considerable quantity of unclassified microorganisms (30%). *Solibacteres* (19%) were mainly represented by microorganisms

Table 1 Mössbauer hyperfine parameters obtained from the Mam Tor ARD sediment and microcosm slurries

Sample/addition	*T*[a]	δ/Fe[b] (mm/s)	Δ[c] (mm/s)	*H*[d] (kOe)	Values reported for α-FeOOH
Before incubation					
ARD sediment	RT	0.38	0.56		δ/Fe = 0.34–0.38 mm/s; Δ = 0.5–0.7 mm/s (Vandenberghe et al. 1986) δ/Fe = 0.38 mm/s; Δ = 0.58 mm/s (Olowe et al. 1990) δ/Fe = 0.37–0.39 mm/s; Δ = 0.54–0.58 mm/s (Herbert 1997)
	LN	0.46	0.73		δ/Fe = 0.47–0.50 mm/s; Δ = 0.65–0.79 mm/s (Larese-Casanova et al. 2010)
		0.48		431	δ/Fe = 0.48–0.49 mm/s; *H* = 432–469 kOe (Goodman and Lewis 1981)
		0.49		462	δ/Fe = 0.47–0.51 mm/s; *H* = 449–495 kOe (Huggins et al. 1983)
After 100 days of incubation					
Plant	LN	0.51		472	δ/Fe = 0.36–0.56 mm/s; *H* = 482–535 kOe (Eissa et al. 1974)
		0.48		444	δ/Fe = 0.45–0.46 mm/s; *H* = 497–504 kOe (Berquó et al. 2007)
Manure	LN	0.49		457	δ/Fe = 0.48 mm/s; *H* = 502 kOe (Bocquet et al. 1992)
		0.50		481	δ/Fe = 0.61–0.62 mm/s; *H* = 500–502 kOe (Brož et al. 1990)
Glycerol	LN	0.51		477	δ/Fe = 0.63–0.69 mm/s; *H* = 495–510 kOe (Dézsi and Fodor 1966)
		0.48		451	*H* = 434–441 kOe (Murad and Bowen 1987)

[a] *T*, temperature (R*T*, room temperature, *LN*, liquid nitrogen temperature)

[b] *δ/Fe*, isomer shift relative to metallic iron

[c] Δ, quadrupole splitting

[d] *H*, hyperfine magnetic field

closely related to the uncultured bacterial clone W2-75. *Alphaproteobacteria* included 9% of organisms closely related to the uncultured clone RS-G2, 4% closely related to the uncultured *Acidisphaera* sp. clone SBLE1E7 and 1% closely related to *Acidiphilum* sp. *NO-17*. *Gammaproteobacteria* represented 17% of the total number of bacterial sequences, most closely related to the uncultured proteobacterial clone *BHL3-310I-54*. This bacterial community is broadly consistent with those reported previously in a range of AMD/ARD sites worldwide (Bond et al. 2000a, b; Johnson et al. 2001; Johnson and Hallberg 2003; Kuang et al. 2013).

3.3 Fe(III) Reduction and Microcosm Geochemistry

A series of microcosm experiments were set up using a variety of carbon sources to determine the effects of natural carbon sources on a range of anaerobic biogeochemical processes, including Fe(III) reduction. Although differences between the contrasting manure treatments were observed (Table S3), analyses generally indicated that manure buffered the pH directly after its addition (from 3.1 to 4.5) and, thereafter, stimulated the slow increase in pH to near-neutral conditions (Fig. 4a). Previous studies already indicated that the alkalinity increased in passive bioreactors used to treat ARD when different types of manure were used (Gibert et al. 2004; Choudhary and Sheoran 2012) and our observations support these observations. The manure additions caused the highest yield of Fe(II) (43 mM) concomitant with a decrease in the redox potential (− 102 mV), lactate accumulation (up to an average of 118 mg/l), a decrease in acetate concentration (Table 2) and, in keeping with the study of Adams et al. (2007), there was an increase in sulfate concentrations (up to 91.5 mM/l).

In the glycerol-amended microcosms, the pH increased moderately, from 3.2 to 3.8 (Fig. 4a; Table 2). The Fe(II) concentration rose to approximately 40 mM, with elevated sulfate concentration (132.3 mM/l), and a slight increase in redox potential (Fig. 4b). Short-chain acids, such as acetate and lactate, were below detection limit (Table 2). In the plant-amended microcosms (Fig. 4a; Table 2), the pH decreased slightly from pH 3.3 to 3.0, probably associated with acetate accumulation (455 mg/l; Table 2). This suggests a depletion of easily degradable organic matter that may be attributed to the presence and stimulation of fermentative microorganisms (Fig. 4; Table 2). In addition, an overall increase in the redox potential, from 403 to 494 mV, was recorded along with increases in the amount of Fe(II) and sulfate (up to an average of 34 mM and 66.7 mM, respectively). In the ‘unamended’ microcosm, the pH also decreased

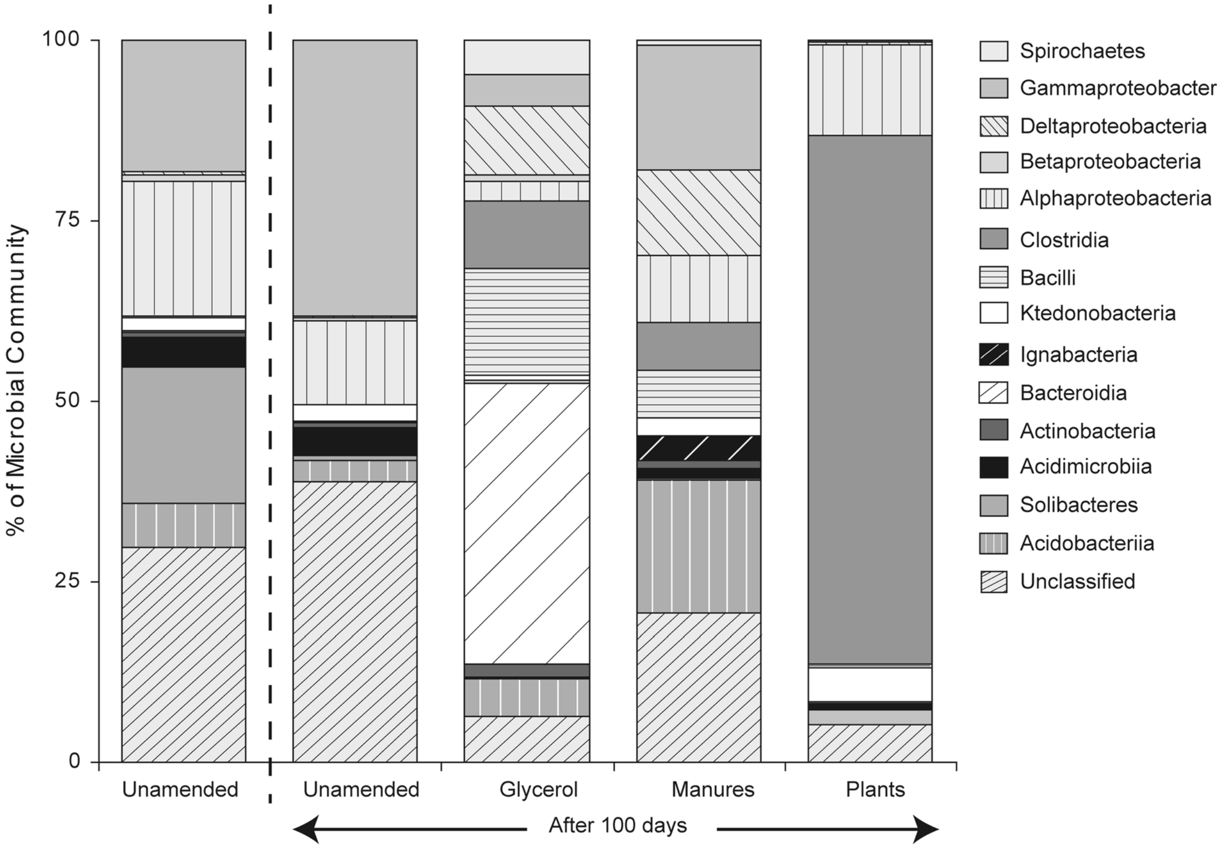

Fig. 3 Relative abundances (%) of dominant bacterial populations present in the Mam Tor ARD sediment and microcosms slurries, stimulated with different organic sources and after 100 days of incubation

slightly (from pH 3.1 to 2.7), associated with lactate accumulation (151 mg/l), while the overall redox potential decreased (from 563 to 495 mV) and a continuous, but less pronounced, increase in the Fe(II) and sulfate concentrations (up to an average of 14 mM and 44.8 mM, respectively) was observed (Fig. 4b; Table 2).

3.4 Impact on Mineralogy

XRD analyses of dried microcosm slurries after 100 days of incubation indicated that goethite was still the dominant mineral phase (Fig. 5a, b and c). In accordance with this, the Mössbauer spectra of all the microcosm slurries were fitted using the characteristic two sextets of goethite (Fig. 5d–f; Table 1). The hyperfine magnetic field values of the microcosm slurries after 100 days of incubation were higher than those calculated for the original ARD sediment, possibly related to an increase in the particle size or the formation of particle clusters (Tamura and Mizushima 2002). Calculation of the crystallite size indicated an increase of the particle size, with a change when manure was used from 41 to 59 nm, on average, and 40 to 45 nm when plant-derived material was added, consistent with the reduced hyperfine magnetic field value reported for the plant-amended microcosm (444 kOe; Table 1). The central doublet in the Mössbauer spectrum of the original ARD sediment (Fig. 2b) attributed to fine particles of goethite, disappeared after incubation (Fig. 5d, e and f), suggesting that fine-particle goethite was bioavailable and consumed during incubation, similar to previous observations of the increased bioavailability of fine-grained iron hydroxide minerals (Pédrot et al. 2011; Cutting et al. 2009).

3.5 Impact on Bacterial Communities Present

To identify which bacteria were stimulated using the different natural electron donors used, bacterial 16S rRNA gene sequences were amplified from selected

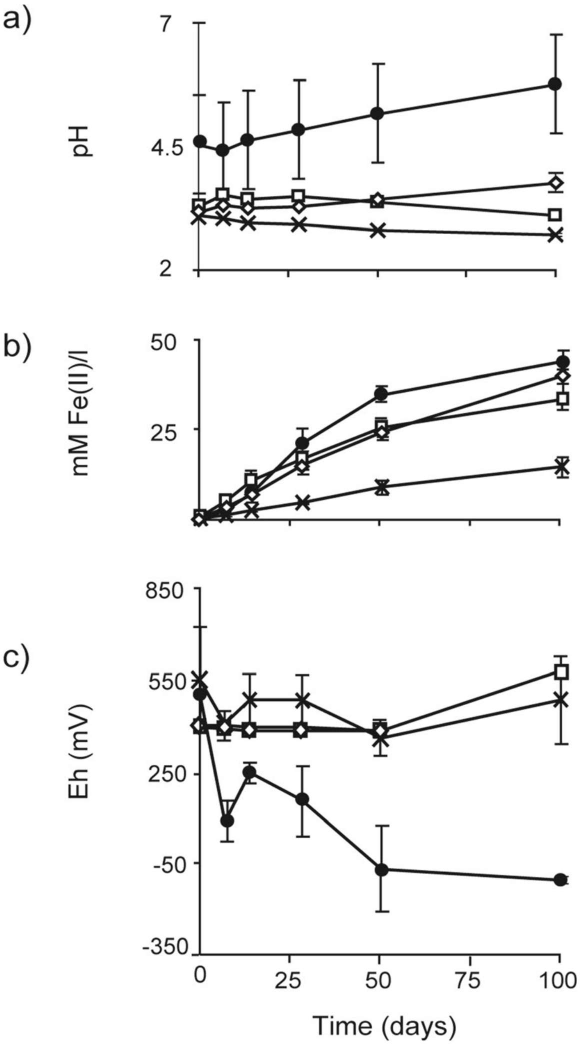

Fig. 4 Geochemical analyses of the aerobic experiments using Mam Tor ARD sediment and different electron donors: **a** pH variation; **b** bioavailable Fe(II) concentrations (mM/l); **c** redox potential. Closed circles, open squares, open diamonds and crosses indicate the manure-, plant- and glycerol-amended microcosms and the control (unamended microcosm), respectively. Bars indicate the error, when they are not visible the error is smaller than the symbol used

microcosm slurries after incubation. For the unamended microcosm, *Gammaproteobacteria* and *Alphaproteobacteria* represented 37% and 17%, respectively, of the total number of bacterial sequences. Microorganisms closely related to the uncultured proteobacterial clone *BHL3-310I-54* doubled in relative abundance after incubation (Fig. 3), consistent with a role in Fe(III) reduction (Whittleston et al. 2011). *Alphaproteobacteria* were represented by organisms affiliated with the uncultured *Acidisphaera* sp. *clone SBLE1E7* (5%) and to the uncultured bacterial clone *RS-G26* (2%). Unclassified microorganisms represented 35% of the total number of sequences, with an abundance of ~ 1%, each.

In the plant-amended microcosms, *Clostridia* (70%) and *Alphaproteobacteria* (13%) were the most abundant microorganisms (Fig. 3). *Clostridia* were chiefly represented by microorganisms closely related to the mesophilic and obligated anaerobe *Clostridium nitrophenolicum strain 1D* (Suresh et al. 2007). *Clostridia* are capable of fermenting or degrading plant polysaccharides, involving the use of enzymes such as cellulases and xylanases (Cornet et al. 1983; Kato et al. 2004; Thomas et al. 2014). Some *Clostridia* have also been detected in acid drainage environments where, for instance, *C. scatologenes SL1* has the capacity to use side chains of aromatic compounds (Küsel and Dorsch 2000). The *Clostridia*-related bacteria are, therefore, probably involved in the degradation of a range of organic compounds derived from the plants supplemented as a carbon source. Other bacteria closely related to *Desulfosporosinus* sp. *clone K1* represented 8% of the total number of sequences. Members of the genus *Desulfosporosinus* are strictly anaerobic, sulfate-reducing bacteria that have the potential for alkali generation and are capable of oxidising a range of organic compounds to acetate (Alazard et al. 2010; Sánchez-Andrea et al. 2013).

The glycerol-amended microcosm was dominated by *Gammaproteobacteria* (16%; Fig. 3) with microorganisms mostly related to the uncultured *Proteobacterial clone BHL3-310I-54*. The addition of glycerol also favoured selection of *Deltaproteobacteria* (12%), represented by microorganisms closely related to the uncultured bacterial clone *CN2m-bac_h7*. *Acidobacteria* included 9% of microorganisms most closely related to the uncultured bacterial clone *W7-15*, 4% of bacteria most closely related to the *Acidisphaera* sp. clone *SBLE1E7* and 3% of bacteria most closely related to the uncultured bacterial clone *WER18*. *Bacilli* closely affiliated to the uncultured *Alicyclobacillus* sp. clone *DAAP3B4* represent approximately 5% of the total sequences; this bacterium is closely related to *Alicyclobacillus ferrooxidans* (NR_044413) and *Alicyclobacillus K23_bac* (EF464642) which have been associated with the oxidation of ferrous iron and sulfate reduction, respectively. Unclassified bacteria represented 21% of the total sequences, with an abundance of less than 3% each.

Table 2 Geochemical data for the microcosms using ARD sediment

Type[a]	Unamended		Glycerol		Plants		Manure	
	0 d	100 d	0 d	100 d	0 d	100 d	0 d	100 d
Fe II (mM/l)	0.5 ± 0.1	14 ± 0.2	0.5 ± 0.1	40 ± 5	0.8 ± 0.4	34 ± 2	0.4 ± 1	43 ± 4
pH	3.1[b]	2.7[b]	3.2[b]	3.8 ± 0.2	3.3[b]	3.0[b]	4.5 ± 0.1	5.8 ± 0.4
Eh (mV)	563 ± 172	495 ± 146	414 ± 0.6	591 ± 5	403 ± 5	494 ± 3	517 ± 87	102 ± 13
Sulfate (mM/l)	9.3 ± 0.2	44.8 ± 1.4	8.2 ± 0.8	132.3 ± 22	12.5 ± 0.4	66.7 ± 3	14.8 ± 3	91.5 ± 27
Lactate (mg/l)[c]	< 0.01	151 ± 6	< 0.01	< 0.01	< 0.01	< 0.01	< 0.01	118 ± 12
Acetate (mg/l)[c]	< 0.01	< 0.01	< 0.01	< 0.1	< 0.1	455 ± 7	18 ± 10	< 0.1
Mg (mg/l)	5 ± 0.3	6 ± 0.8	47 ± 0.2	44 ± 0.8	60 ± 0.5	59 ± 7.0	10 ± 0.7	14 ± 2
Mn (mg/l)	1.2[b]	1.5[b]	11[b]	12[b]	14[b]	17 ± 1.3	1.1 ± 0.4	1.7 ± 0.6
Organic analyses								
OM (%)[d]	14.3 ± 0.1	14.6 ± 0.1 (0)	14.3 ± 0.1	14.2[b] (0)	18.8 ± 1.1	18.2 ± 0.9 (3)	19.0 ± 0.1	18.5 ± 0.8 (3)
HMW *n*-alkanes (μg/g sed)[e,f]	3.3	3.3 (0)	4.6	2.5 (46)	4.7–12.5	1.2–2.7 (74 ± 10)	5.2–25	4.5–23 (14 ± 7)
HMW *n*-alkanols (μg/g sed)[e,f]	2.9	2.8 (3)	2.8	0.6 (79)	3.9–4.6	3.3–4.1 (12 ± 14)	8.6–86	5.9–84 (76 ± 15)
Steroids (μg/g sed)[f,g]	9.8	8.9 (9)	5.1	1.1 (78)	4.3–9.9	3.5–5.2 (27 ± 22)	46–64	38–55 (11 ± 9)

[a] 0 d = conditions at start of experiment, 100 d = conditions after 100 days incubation

[b] Value variation < 0.1 units

[c] Values below the typical routine detection limits (0.01–0.1 mg/l) reported as < 0.01

[d] Total organic matter

[e] HMW, high molecular weight, summed concentration over the range C_{20}–C_{31}

[f] Values reported as a range, values between brackets are percentage of the original concentrations lost after 100 days

[g] Summed concentrations of C_{27} to C_{30} stanols and $C_{27:1}$, $C_{28:1}$, $C_{28:2}$, $C_{29:1}$ and $C_{29:2}$ sterols

For the manure-amended microcosms (Fig. 3), *Bacteroidia* represented the largest portion of the 16S rRNA gene library. The most abundant sequence was closely related to the uncultured *Paludibacter* sp. *clone 17-13* (32%). *Paludibacter* sp. are fermentative bacteria with members that have also been identified in acid drainage environments and in AMD bioreactors amended with complex organic substrates (Lindsay et al. 2011; Sánchez-Andrea et al. 2013). The most abundant *Bacilli* were highly represented by the *Alicyclobacillus* sp. *clone DAAP3B4*, 9% of the total sequences. Some *Alicyclobacilli* are able to reduce Fe(III) (Bridge and Johnson 1998) and others such as *Alicyclobacillus Y004* are strict heterotrophs, able to grow at pH values down to 1 (Johnson et al. 2003). *Deltaproteobacteria* were mainly represented (6%) by a microorganism closely related to *Desulfovibrio idahonensis CY2*. Members of the *Desulfovibrio* family are well known to oxidise organic carbon coupled with the reduction of sulfate (Reichenbecher and Schink 1997, Abildgaard et al. 2006), which could be released via the reduction of Fe(III) sulfate minerals (Adams et al. 2007) and can also be introduced via the addition of manure (Cocos et al. 2002). It should be noted that *D. idahonensis CY2* could be involved in microbial Fe(III)-reduction, although this process is not sufficient to support its growth (Sass et al. 2009).

Of the total 16S rRNA genes detected, 2% were closely related to the uncultured *Geobacteraceae clone M22_1334*. *Geobacter* species are important metal-reducing microorganisms given their ability to couple the reduction of Fe(III) (or other metals) to the complete oxidation of organic compounds (Lovley et al. 1993; Zhang et al. 2012; Orellana et al. 2013). Other detected bacteria included microorganisms closely related to the *Acidobacterial* clone *T7_12* (2%) and the uncultured *Spirochaetaceae bacterial* clone *L6-D1* (3%), which has been detected in sulfate-reducing bioreactors (Koschorreck et al. 2010).

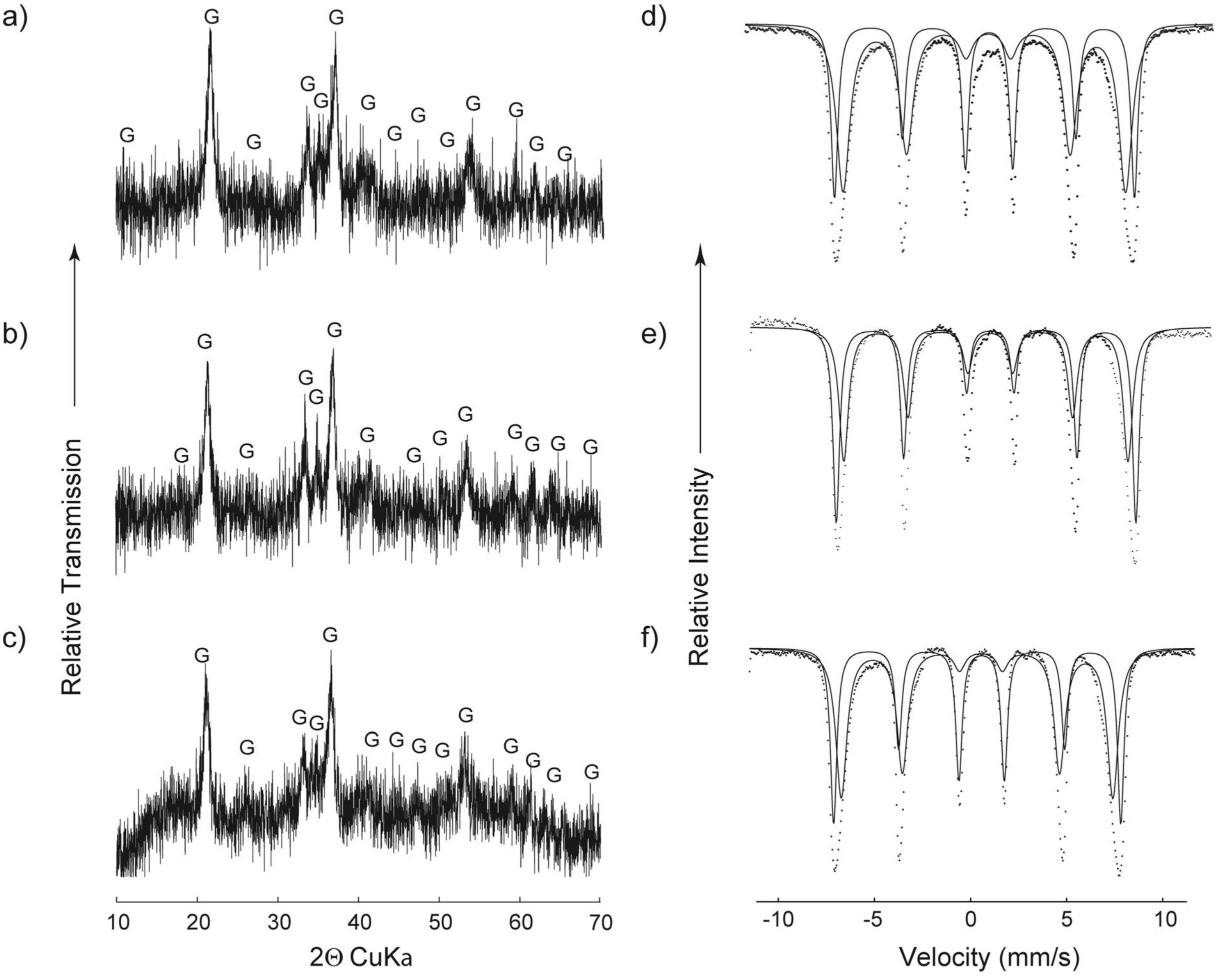

Fig. 5 X-ray diffractograms (left) and Mössbauer spectra at liquid nitrogen temperature (right) of Mam Tor ARD microcosm slurries after 100 days of incubation. Analysis of microcosms using (**a**) and (**d**) plant material; (**b**) and (**e**) manure; and (**c**) and (**f**) glycerol. The XRD analyses show that goethite (G) is the dominant mineral phase and the Mossbauer spectra are consistent with this interpretation

3.6 Impact on Organic Composition

Analysis of the organic matter content of the microcosm slurries after 100 days of incubation indicated a very low overall loss (up to 3%) of organic matter during incubation (Table 2). However, although lipids are only a relatively small part of the overall organic matter present, lipid analyses of the slurries suggest some compound modifications between the different treatments. The unamended microcosms showed no significant differences between the amounts of lipids present before and after incubation, with losses varying between 0% (HMW *n*-alkanes) and 9% (steroids). By contrast, the differences for the other microcosms were substantial; most notable were the changes for the glycerol-amended microcosms, with losses ranging from 46% for the HMW *n*-alkanes up to 79% for the HMW *n*-alkanols. The addition of glycerol seems to have stimulated the microbial community in such a way that some of the original, plant-derived material already present in the sediment was utilised.

Lipid analyses of the plant- and manure-amended microcosm slurries also indicated substantially lower amounts of lipids after 100 days of incubation when compared with their initial concentrations (Table 2). In the plant microcosms, an elevated level of lipid degradation was observed with losses ranging from 12 to 74% (Table 2) but this was not related to an increase in pH and seemed not to stimulate microbial Fe(III) reduction, probably due to the accumulation of acetate, inhibiting microbial Fe(III) reduction at low pH (Küsel and Dorsch 2000). Elevated levels of lipid degradation, with losses between 11 and 76% (Table 2), were also noted in the manure-supplemented microcosms where the maximum pH amelioration and Fe(III) reduction rates were recorded. The distribution patterns undoubtedly indicate that the HMW *n*-alkanes and *n*-alkanols from the manure additions are of higher plant origin (Table S4), probably originating from the feeding products given to the animals that produced the manures.

Additional py-GC-MS analyses of a subset of the microcosm slurries also indicated some variations in the macromolecular compositions between the original compositions and those after 100 days of incubation (Fig. 6; Table S5). Analyses of the manure-amended microcosms before and after incubation indicated a substantial drop in the relative contribution of lignin compounds of 8% (from 33 to 25% of total), while the relative amounts of phenols increased (+ 5%) and the relative amounts of the other compound classes remained unchanged (Fig. 5 and Table S5). Relatively large amounts of lactate were observed at the end of the incubation (Table 2) suggesting the presence of potential Fe(III) reducers capable of utilising a range of complex organics (Küsel and Dorsch 2000). The substantial drop in the relative amounts of lignin suggests that in these microcosms lignin or other substrates exposed due to the modification of lignin could be the source of organic carbon used. However, more research is needed to confirm this interpretation.

In the unamended microcosms, the original macromolecular composition was dominated by polysaccharides (44%) with substantial contributions from lignin-derived moieties and nitrogen-containing compounds (19% and 17%, respectively). After incubation, polysaccharides and nitrogen compounds (57% and 26%, respectively) dominate and comparable with the manure-amended microcosms, the biggest drop in relative contribution was observed for the lignin compounds (− 8%; Fig. 6 and Table S5). The plant-amended microcosm was dominated by polysaccharide moieties (32–57%), nitrogen-containing compounds (10–21%) and in the case of reed-amended microcosm, lignin moieties (37%). The same compound classes dominated the composition after incubation (polysaccharide moieties 27–72%; nitrogen-containing compounds 12–14%; lignin 40%; Fig. 6 and Table S5). However, in contrast to the manure-amended microcosm to relative contribution of lignin, moieties did not decrease in the relative contribution, suggesting that the lignin from the reed was not as bioavailable as in the manure-amended microcosms.

The combined results indicate that the biogeochemical changes in the microcosms were dictated by the type of

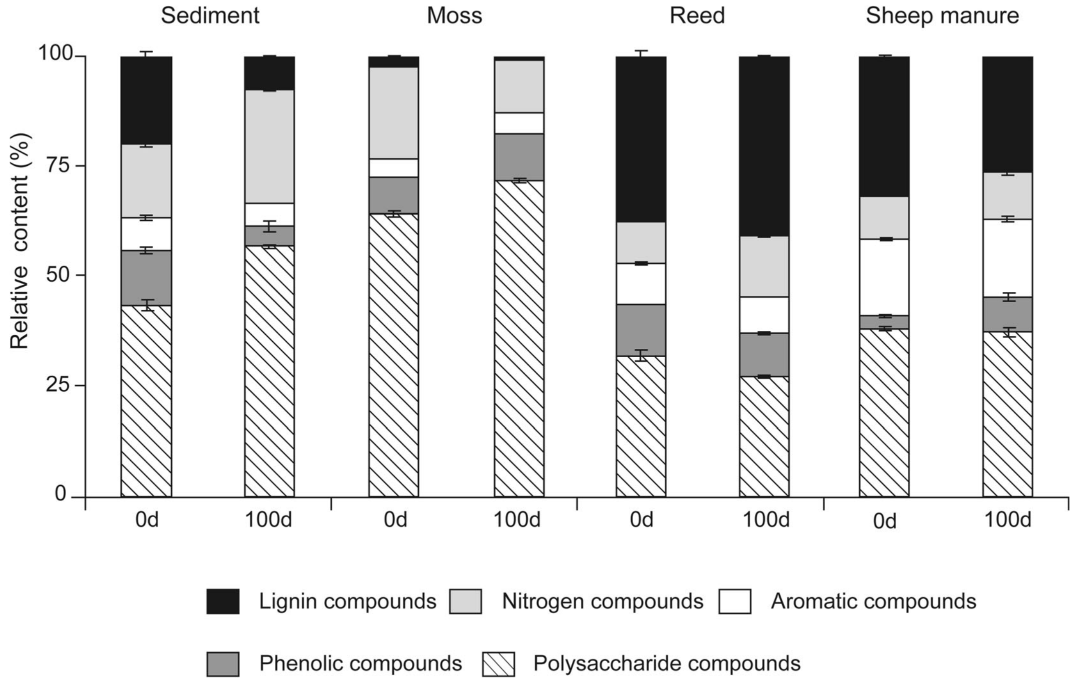

Fig. 6 Macromolecular groups obtained from the pyrolysates of the microcosms supplemented with different carbon sources. The contribution of each group is given in relative abundance. 0d = before incubation; 100d = after 100 days incubation

amendment used, suggesting that (i) the organic fractions of the plant and manure additions are not evenly bioavailable and (ii) the addition of diverse carbon sources promotes the metabolism of microorganisms which can fuel a range of geomicrobial processes, including iron and sulfate reduction (Adams et al. 2007; Church et al. 2007, Choudhary and Sheoran 2012; Johnson et al. 2012; Yamada et al. 2014). The experiments support previous work (Choudhary and Sheoran 2012) suggesting that the addition of the optimal carbon source is a key factor in developing a targeted "biostimulation" remediation strategy for sites impacted by acid rock or mine drainage.

4 Conclusions

The microcosm-based experiments using Mam Tor ARD sediments have shown that the bioavailability of the fine-sized fraction of goethite and the use of manure as carbon source can stimulate microbial alkali-generation processes coupled with the degradation of organic matter. This finding may offer a bioremediation strategy for ARD, due to the potential efficiency of manure in passive treatments and its economic viability. However, more research is needed to identify the bacteria involved in the microbial processes, and to better understand the natural attenuation processes. In addition, although this study has focused on iron reduction, it demonstrates that the use of the optimal natural carbon source is important and can promote the metabolism of microorganisms which can fuel a range of geomicrobial processes. This includes the stimulation of sulfate reduction in lower Fe systems that could also result in generation of alkalinity and metal removal through sulfidation reactions.

Acknowledgements We thank the late P. Wincott for his help and advice on Mössbauer Spectrometry; C. Davies, P. Lythgoe and A. Bewsher for their assistance in chemical analyses.

Authors' Contributions All authors contributed to the study conception and design and all authors commented on previous versions of the manuscript. All authors read and approved the final manuscript.

Funding PhD studentship for MEJC, funded by CONACyT-Mexico (308702).Data AvailabilityNot applicable.

Compliance with Ethical Standards

Conflict of Interest The authors declare that they have no conflict of interest.

Code Availability Not applicable.

References

Abildgaard, L., Nielsen, M.B., Kjeldsen, K.U. and Ingvorsen, K. (2006) Alkalitolerans sp. nov., a novel alkalitolerant, sulphate-reducing bacterium isolated from district heating water. *International Journal of Systematic and Evolutionary Microbiology 55*, 1019–1024.

Adams, L. K., Harrison, J. M., Lloyd, J. R., Langley, S., & Fortin, D. (2007). Activity and diversity of Fe(III)-reducing bacteria in a 3000-year-old acid mine drainage site analogue. *Geomicrobiology Journal, 24*, 295–305.

Alazard, D., Joseph, M., Battaglia-Brunet, F., Cayol, J. L., & Ollivier, B. (2010). Desulfosporosinus acidiphilus sp. nov.: a moderately acidophilic sulfate-reducing bacterium isolated from acid mining drainage sediments. *Extremophiles, 14*, 305–312.

Allen, J.R.L. (1960) The Mam Tor Sandstones: A "turbidite" facies of the Namurian deltas of Derbyshire, England. *Journal of Sedimentary Research30*, 193–208.

Bassil, N. M., Bryan, N., & Lloyd, J. R. (2015). Microbial degradation of isosaccharinic acid at high pH. *ISME Journal, 9*, 310–320.

Beaudoin, A. (2003). A comparison of two methods for estimating the organic content of sediments. *Journal of Paleolimnology, 29*, 387–390.

Berquó, T., Imbernon, R., Blot, A., Franco, D., Toledo, M., & Partiti, C. (2007). Low temperature magnetism and Mössbauer spectroscopy study from natural goethite. *Physics and Chemistry of Minerals, 34*, 287–294.

Blumer, M. (1957). Removal of elemental sulfur from hydrocarbon fractions. *Analytical Chemistry, 29*, 1039–1041.

Bocquet, S., Pollard, R., & Cashion, J. (1992). Dynamic magnetic phenomena in fine-particle goethite. *Physical Review B, 46*, 11657.

Bond, P. L., Druschel, G. K., & Banfield, J. F. (2000a). Comparison of acid mine drainage microbial communities in physically and geochemically distinct ecosystems. *Applied and Environmental Microbiology, 66*, 4962–4971.

Bond, P. L., Smriga, S. P., & Banfield, J. F. (2000b). Phylogeny of microorganisms populating a thick, subaerial, predominantly lithotrophic biofilm at an extreme acid mine drainage site. *Applied and Environmental Microbiology, 66*, 3842–3849.

Bridge, T. A. M., & Johnson, D. B. (1998). Reduction of soluble iron and reductive dissolution of ferric iron-containing minerals by moderately thermophilic iron-oxidizing bacteria. *Applied and Environmental Microbiology, 64*, 2181–2186.

Brož, D., Straková, J., Šubrt, J., Vinš, J., Sedlák, B., & Reiman, S. I. (1990). Mössbauer spectroscopy of goethite of small particle size. *Hyperfine Interactions, 54*, 479–482.

Choudhary, R. P., & Sheoran, A. S. (2012). Performance of single substrate in sulphate reducing bioreactor for the treatment of acid mine drainage. *Minerals Engineering, 39*, 29–35.

Church, C.D., Wilkin, R.T., Alpers, C.N. et al. (2007) Microbial sulfate reduction and metal attenuation in pH 4 acid mine water. *Geochemical Transactions 8*, 10.

Cocos, I. A., Zagury, G. J., Clément, B., & Samson, R. (2002). Multiple factor design for reactive mixture selection for use in reactive walls in mine drainage treatment. *Water Research, 36*, 167–177.

Cornet, P., Millet, J., Beguin, P., & Aubert, J. P. (1983). Characterization of two cel (cellulose degradation) genes of *Clostridium Thermocellum* coding for endoglucanases. *Nature Biotechnology, 1*, 589–594.

Costa, M. C., & Duarte, J. C. (2005). Bioremediation of acid mine drainage using acidic soil and organic wastes for promoting sulphate-reducing bacteria activity on a column reactor. *Water, Air, and Soil Pollution, 165*, 325–345.

Cutting, R. S., Coker, V. S., Fellowes, J. W., Lloyd, J. R., & Vaughan, D. J. (2009). Mineralogical and morphological constraints on the reduction of Fe(III) minerals by *Geobacter sulfurreducens*. *Geochimica et Cosmochimica Acta, 73*, 4004–4022.

Dézsi, I., & Fodor, M. (1966). On the antiferromagnetism of α-FeOOH. *Physica Status Solidi (b), 15*, 247–254.

Dickson, L., Bull, I. D., Gates, P. J., & Evershed, R. P. (2009). A simple modification of a silicic acid lipid fractionation protocol to eliminate free fatty acids from glycolipid and phospholipid fractions. *Journal of Microbiological Methods, 78*, 249–254.

Eissa, N. A., Sallam, H. A., Gomaa, S. S., Saleh, S. A., & Miligy, Z. (1974). Mössbauer study of Egyptian goethite. *Journal of Physics D: Applied Physics, 7*, 2121.

Ford, T., Sarjeant, W. and Smith, M. (1993). Minerals of the Peak District. *Bulletin of the Peak District Mines Historical Society 12*, 1.

Gibert, O., J. de Pablo, J. L. Cortina and C. Ayora (2005). Sorption studies of Zn(II) and Cu(II) onto vegetal compost used on reactive mixtures forin situ treatment of acid mine drainage. *Water Research 39*(13): 2827–2838.

Golden, D. C., Bowen, L. H., Weed, S. B., & Bigham, J. M. (1979). Mössbauer studies of synthetic and soil-occurring aluminum-substituted goethites. *Soil Science Society of America Journal, 43*, 802–808.

Goodman, B. A., & Lewis, D. G. (1981). Mössbauer spectra of aluminious goethites (α-FeOOH). *Journal of Soil Science, 32*, 351–364.

Heiri, O., Lotter, A., & Lemcke, G. (2001). Loss on ignition as a method for estimating organic and carbonate content in sediments: reproducibility and comparability of results. *Journal of Paleolimnology, 25*, 101–110.

Herbert, R. B. (1997). Properties of goethite and jarosite precipitated from acidic groundwater, Dalarna, Sweden. *Clays and Clay Minerals, 45*, 261–273.

Huggins, F. E., Huffman, G. P., & Lin, M. C. (1983). Observations on low-temperature oxidation of minerals in bituminous coals. *International Journal of Coal Geology, 3*, 157–182.

Johnson, D. B. (1998). Biodiversity and ecology of acidophilic microorganisms. *FEMS Microbiology Ecology, 27*, 307–317.

Johnson, D. B., & Hallberg, K. B. (2003). The microbiology of acidic mine waters. *Research in Microbiology, 154*, 466–473.

Johnson, D. B., Rolfe, S., Hallberg, K. B., & Iversen, E. (2001). Isolation and phylogenetic characterization of acidophilic microorganisms indigenous to acidic drainage waters at an abandoned Norwegian copper mine. *Environmental Microbiology, 3*, 630–637.

Johnson, D. B., Okibe, N., & Roberto, F. (2003). Novel thermo-acidophilic bacteria isolated from geothermal sites in Yellowstone National Park: physiological and phylogenetic characteristics. *Archives of Microbiology, 180*(1), 60–68.

Johnson, D. B., Kanao, T., & Hedrich, S. (2012). Redox transformations of iron at extremely low pH: fundamental and applied aspects. *Frontiers in Microbiology, 3*, 96.

Kato, S., Haruta, S., Cui, Z. J., Ishii, M., & Igarashi, Y. (2004). Effective cellulose degradation by a mixed culture system composed of a cellulolytic *Clostridium* and aerobic non-cellulolytic bacteria. *FEMS Microbiology Ecology, 51*, 133–142.

Kim, G. M., Kim, D. H., Kang, J. S., & Baek, H. (2014). Treatment of synthetic acid mine drainage using rice wine waste as a carbon source. *Environmental Earth Sciences, 71*, 4603–4609.

Koschorreck, M., Geller, W., Neu, T., Kleinsteuber, S., Kunze, T., Trosiener, A., & Wendt-Potthoff, K. (2010). Structure and function of the microbial community in an in situ reactor to treat an acidic mine pit lake. *FEMS Microbiology Ecology, 73*, 385–395.

Kuang, J. L., Huang, L. N., Chen, L. X., Hua, Z. S., Li, S. J., Hu, M., Li, J. T., & Shu, W. S. (2013). Contemporary environmental variation determines microbial diversity patterns in acid mine drainage. *ISME Journal, 7*, 1038–1050.

Küsel, K., & Dorsch, T. (2000). Effect of supplemental electron donors on the microbial reduction of Fe(III), sulfate, and CO_2 in coal mining–impacted freshwater lake sediments. *Microbial Ecology, 40*, 238–249.

Larese-Casanova, P., Cwiertny, D. M., & Scherer, M. M. (2010). Nanogoethite formation from oxidation of Fe(II) sorbed on aluminum oxide: implications for contaminant reduction. *Environmental Science & Technology, 44*, 3765–3771.

Liao, J., Wen, Z., Ru, X., Chen, J., Wu, H., & Wei, C. (2016). Distribution and migration of heavy metals in soil and crops affected by acid mine drainage: Public health implications in Guangdong Province, China. *Ecotoxicology and Environmental Safety, 124*, 460–469.

Lindsay, M. B. J., Wakeman, K. D., Rowe, O. F., Grail, B. M., Ptacek, C. J., Blowes, D. W., & Johnson, D. B. (2011). Microbiology and geochemistry of mine tailings amended with organic carbon for passive treatment of pore water. *Geomicrobiology Journal, 28*, 229–241.

Lovley, D. R., & Phillips, E. J. (1986). Organic matter mineralization with reduction of ferric iron in anaerobic sediments. *Applied and Environmental Microbiology, 51*, 683–689.

Lovley, D. R., Giovannoni, S. J., White, D. C., Champine, J. E., Phillips, E. J. P., Gorby, Y. A., & Goodwin, S. (1993). *Geobacter metallireducens gen. nov. sp. nov.*, a microorganism capable of coupling the complete oxidation of organic compounds to the reduction of iron and other metals. *Archives of Microbiology, 159*, 336–344.

Moeng, K. (2019). Community perceptions on the health risks of acid mine drainage: the environmental justice struggles of communities near mining fields. *Environment, Development and Sustainability, 21*(6), 2619–2640.

Mørup, S., Topsøe, H., & Clausen, B. S. (1982). Magnetic properties of microcrystals studied by Mössbauer spectroscopy. *Physica Scripta, 25*, 713.

Murad, E. (1989) Poorly-crystalline minerals and complex mineral assemblages. *Hyperfine Interactions 47–48*, 33–53.

Murad, E., & Bowen, L. H. (1987). Magnetic ordering in Al-rich goethites; influence of crystallinity. *American Mineralogist, 72*, 194–200.

Olowe, A. A., Refait, P., & Génin, J. M. R. (1990). Superparamagnetic behaviour of goethite prepared in sulphated medium. *Hyperfine Interactions, 57*, 2037–2043.

Orellana, R., Leavitt, J. J., Comolli, L. R., Csencsits, R., Janot, N., Flanagan, K. A., Gray, A. S., Leang, C., Izallalen, M., Mester, T., & Lovley, D. R. (2013). U(VI) reduction by diverse outer surface c-type cytochromes of *Geobacter sulfurreducens*. *Applied and Environmental Microbiology, 79*, 6369–6374.

Pédrot, M., Boudec, A. L., Davranche, M., Dia, A., & Henin, O. (2011). How does organic matter constrain the nature, size and availability of Fe nanoparticles for biological reduction? *Journal of Colloid and Interface Science, 359*, 75–85.

Queiroz, H. M., Nóbrega, G. N., Ferreira, T. O., Almeida, L. S., Romero, T. B., Santaella, S. T., Bernardino, A. F., & Otero, X. L. (2018). The Samarco mine tailing disaster: a possible time-bomb for heavy metals contamination? *Science of the Total Environment, 637-638*, 498–506.

Reichenbecher, W. and Schink, B. (1997) Desulfovibrio inopinatus, sp. nov., a new sulfate-reducing bacterium that degrades hydroxyhydroquinone (1,2,4-trihydroxybenzene). *Archives of Microbiology 169*, 88.

Rimstidt, J. D., & Vaughan, D. J. (2003). Pyrite oxidation: a state-of-the-art assessment of the reaction mechanism. *Geochimica et Cosmochimica Acta, 67*, 873–880.

Rutter, E. H., & Green, S. (2011). Quantifying creep behaviour of clay-bearing rocks below the critical stress state for rapid failure: Mam Tor landslide, Derbyshire, England. *Journal of the Geological Society, 168*, 359–372.

Sánchez-Andrea, I., Stams, A. J. M., Amils, R., & Sanz, J. L. (2013). Enrichment and isolation of acidophilic sulfate-reducing bacteria from Tinto River sediments. *Environmental Microbiology Reports, 5*, 672–678.

Sass, H., Ramamoorthy, S., Yarwood, C., Langner, H., Schumann, P., Kroppenstedt, R. M., Spring, S., & Rosenzweig, R. F. (2009). *Desulfovibrio idahonensis sp. nov.*, sulfate-reducing bacteria isolated from a metal(loid)-contaminated freshwater sediment. *International Journal of Systematic and Evolutionary Microbiology, 59*, 2208–2214.

Singer, P. C., & Stumm, W. (1970). Acidic mine drainage: the rate-determining step. *Science, 167*, 1121–1123.

Skempton, A. W., Leadbeater, A. D., and Chandler, R. J. (1989) The Mam Tor landslide, North Derbyshire. Philosophical transactions of the Royal Society of London. Series A, Mathematical and Physical Sciences 329, 503–547.

Stookey, L. L. (1970). Ferrozine -a new spectrophotometric reagent for iron. *Analytical Chemistry, 42*, 779–781.

Suresh, K., Prakash, D., Rastogi, N., & Jain, R. K. (2007). *Clostridium nitrophenolicum sp. nov.*, a novel anaerobic p-nitrophenol-degrading bacterium, isolated from a subsurface soil sample. *International Journal of Systematic and Evolutionary Microbiology, 57*, 1886–1890.

Tamura, I., & Mizushima, T. (2002). Explanation for magnetic properties of interacting iron oxide nanocrystals. *Journal of Magnetism and Magnetic Materials, 250*, 241–248.

Thomas, L., Joseph, A., & Gottumukkala, L. D. (2014). Xylanase and cellulase systems of *Clostridium sp.*: An insight on molecular approaches for strain improvement. *Bioresource Technology, 158*, 343–350.

van der Kraan, A. M., & van Loef, J. J. (1966). Superparamagnetism in submicroscopic α-FeOOH particles observed by the Mössbauer effect. *Physics Letters, 20*, 614–616.

Vandenberghe, R., De Grave, E., De Geyter, G., & Landuydt, C. (1986). Characterization of goethite and hematite in a Tunisian soil profile by Mössbauer spectroscopy. *Clays and Clay Minerals, 34*, 275–280.

Vear, A., & Curtis, C. (1981). A quantitative evaluation of pyrite weathering. *Earth Surface Processes and Landforms, 6*, 191–198.

Waltham, A. C., & Dixon, N. (2000). Movement of the Mam Tor landslide, Derbyshire, UK. *Quarterly Journal of Engineering Geology and Hydrogeology, 33*, 105–123.

Whittleston, R. A., Stewart, D. I., Mortimer, R. J. G., Tilt, Z. C., Brown, A. P., Geraki, K., & Burke, I. T. (2011). Chromate reduction in Fe(II)-containing soil affected by hyperalkaline leachate from chromite ore processing residue. *Journal of Hazardous Materials, 194*, 15–23.

Williamson, A. J., Morris, K., Shaw, S., Byrne, J. M., Boothman, C., & Lloyd, J. R. (2013). Microbial reduction of Fe(III) under alkaline conditions relevant to geological disposal. *Applied and Environmental Microbiology, 79*, 3320–3326.

Yamada, C., Kato, S., Kimura, S., Ishii, M., & Igarashi, Y. (2014). Reduction of Fe(III) oxides by phylogenetically and physiologically diverse thermophilic methanogens. *FEMS Microbiology Ecology, 89*, 637–645.

Zhang, T., Bain, T. S., Nevin, K. P., Barlett, M. A., & Lovley, D. R. (2012). Anaerobic benzene oxidation by *Geobacter* species. *Applied and Environmental Microbiology, 78*, 8304–8310.